

Blueshift of surface plasmon resonance spectra in anneal-treated silver nanoslit arrays

Yun Suk Jung, Zhijun Sun, and Hong Koo Kim^{a)}

Department of Electrical and Computer Engineering and Institute of NanoScience and Engineering, University of Pittsburgh, Pittsburgh, Pennsylvania 15261

Jean Blachere

Department of Materials Science and Engineering, University of Pittsburgh, Pittsburgh, Pennsylvania 15261

(Received 7 June 2005; accepted 8 November 2005; published online 28 December 2005)

Silver nanoslit arrays were anneal treated in vacuum, and the effects on the surface morphology of silver and the surface plasmon resonance characteristics were investigated. Optical transmission through nanoslit arrays shows a distinctive change in the spectral profiles after annealing: A clear blueshift of the transmission peaks and dips (20 nm shift for an anneal temperature of 150 °C). Scanning electron microscopy reveals a morphological change of silver: Increased grain sizes, and smooth and round surface profiles after the anneal treatment. The observed blueshift of transmission spectra correlates well with the geometrical and dimensional changes of silver islands defined between slits, which are found to alter the surface plasmon resonance conditions involving various mechanisms in different regimes. © 2005 American Institute of Physics. [DOI: 10.1063/1.2159095]

Interactions of light with metal nanoslit arrays produce many interesting phenomena and have been the subject of extensive studies.^{1–6} Essential to understanding the overall phenomena is to elucidate the mechanisms of surface plasmon (SP) interactions with the metal structure. Transmission of light through metal nanoslit arrays, for example, shows characteristic spectra with clear peaks and dips. We recently reported that the metal nanoslit array structures support various different modes of surface plasmon resonance involving different sections of metal surfaces.^{7,8} The SP resonance points are found to correspond to the dips and peaks of the transmission spectra. The SP waves localized to each metal island can also interact with neighboring ones via near-field coupling across the slit, and this can significantly alter the transmission spectra.⁷

In this letter, we report our further study of the plasmonic phenomena occurring in silver nanoslit array structures. We have investigated the effects of thermal annealing on the surface plasmon resonance characteristics in the arrays. The spatial extension of SP waves is usually an order of magnitude smaller than the wavelength along the propagation direction.⁹ The array structures were designed to span nano- to micrometer length scales in feature sizes, i.e., the slit width of the 10 nm order and the grating period of the 100 nm order. This is to accommodate the interactions of waves (plasmonic and photonic) with the structure involving different length scales. The metal nanoslit arrays were formed by angle deposition of silver on mesa-etched quartz substrates. Anneal treatment of a deposited metal film is expected to alter the microstructure of metal (such as grain boundaries, surface roughness, etc.) and the size and shape of each metal island separated by slits, and thus the gap between them (i.e., slit width). This annealing-induced change of metal that may occur at nano- to microscale is expected to sensitively affect the SP interactions with the metal.

The silver nanoslit arrays used in this study were fabricated using a holographic lithography and plasma etching

technique in conjunction with angle deposition of metal (see Ref. 7 for experiment details.) Grating periods are designed to be 400 nm, and slit width in the range of 50–120 nm. The metal thickness is controlled to be 200 nm. The Ag-deposited sample was then cut into two pieces and one was anneal treated in vacuum (1×10^{-6} Torr) for 30 min at 150 °C. Figure 1 shows scanning electron microscope (SEM) images of an as-deposited Ag nanoslit array sample. Well-defined quartz mesas are revealed with sharp edges and flat top and sidewalls profiles [Fig. 1(a)]. The silver layer was deposited on mesas with an evaporation flux incident from the left-hand side of mesas with tilt angle of 45°. The SEM image shows a conformal profile of Ag surface, i.e., an inverted “L” shape with a relatively sharp edge at the left-hand side of the top surface. The amount of metal deposited on the left sidewall of mesas is nearly the same as that on the mesa top, a result consistent with the angle deposition condition described above. The gap between Ag islands is estimated to be around 30 nm. Figure 1(b) shows a plan-view image of the same sample. The surface morphology of as-deposited Ag reveals many grain boundaries in each metal island (with grain size typically on the order of 10 nm). The granular structure is commonly observed in deposited metal films. (The apparent wide opening of the gap between Ag islands in this plan-view image is an artifact caused by the location of the detector to the left of the sample, essentially a shadow effect).¹⁰

Figures 1(c) and 1(d) show SEM images of the anneal-treated sample. Annealing of Ag, performed at the relatively mild temperature (150 °C), is found to induce significant changes in the morphology of metal. The grain sizes grew to 50–100 nm range, and some grains are over 200 nm, showing a “bamboo” structure along the mesa [Fig. 1(d)]. Figure 1(c) shows another major change in the cross-sectional profile: The initially conformal profile of metal surface became round and smooth after annealing. (This cross section was obtained by cleaving the anneal-treated sample.) It is interesting to note that the bottom edge of metal deposited on the right-hand sidewall of mesas also became round. This indi-

^{a)}Electronic mail: kim@engr.pitt.edu

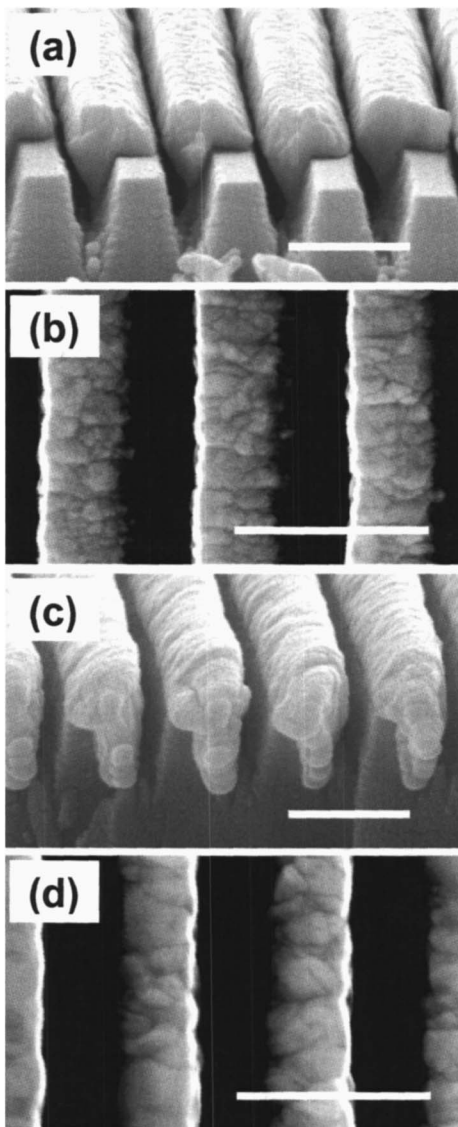


FIG. 1. SEM micrographs of a silver nanoslit array structure formed on a mesa-etched quartz substrate: The effects of annealing (at 150 °C in a vacuum for 30 min) on the morphology of metal. (a) Side view of an as-deposited sample. (b) Top view of an as-deposited sample. (c) Side view of an anneal-treated sample. (d) Top view of an anneal-treated sample. The scale bar is 500 nm.

icates that dewetting of metal on silica surface occurs even at this relatively low temperature of annealing. [Note that the Ag layer was deposited with an evaporation flux incident from the right hand of mesas in this image shown in Fig. 1(c), and the as-deposited Ag shows extremely small contact angle in the bottom edge as shown in Fig. 1(a).] Grain growth and dewetting can be explained by the tendency of metal to minimize its surface energies.¹¹ Grain growth can occur through motion of grain boundaries, which results in the shrinkage and elimination of small grains, and an eventual increase in the average grain size of the remaining grains. Wetting depends on the relative surface and interface energies. Dewetting of a film can occur at the film edges during annealing if the surface energy of a substrate is smaller than the sum of the surface and interface energies of a film. Diffusivity of material is a strong function of temperature, and as such both grain growth and dewetting processes are expected to show similar dependency. 150 °C anneal temperature corresponds to the homologous tempera-

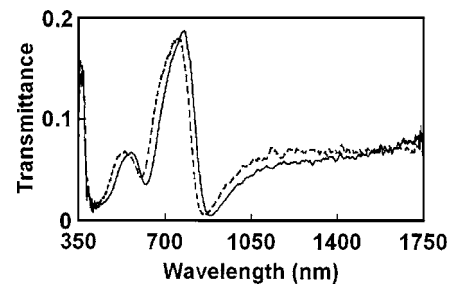


FIG. 2. Transmission spectra of a silver nanoslit array structure shown in Fig. 1: As deposited (solid curve), and after anneal treatment in vacuum (dashed curve).

ture of 0.34 K, which is defined as the temperature in degrees K divided by the melting temperature (also in degrees K) of the material under consideration. In thin-film studies of Ag, it has been known that grain boundary motion plays an important role in grain growth even at homologous temperatures as low as 0.2 K.¹¹ Overall, the densification (resulting from grain growth) and the shape change (round edges and circular cross sections caused by the grain growth and dewetting) increased the slit width to 50 to 80 nm range.

Figure 2 shows optical transmission through the Ag nanoslit arrays before and after the anneal treatment. An unpolarized white light was incident normal to the substrate surface. The zeroth order transmission through the Ag nanoslit array was collected and analyzed with an optical spectrum analyzer. The peak transmission of an unpolarized light is measured to be around 20%. (When normalized for a TM polarized light, the transmission would be two times this value, i.e., 40% transmission for TM polarization.) The transmission spectra show a clear blueshift after the anneal treatment, although the transmittance basically remains at the same level. The transmission peak at 780 nm of the as-deposited sample, for example, shifted to 760 nm, and a similar amount of shift with the minor peak at 560 nm, and the dips at 620 nm and 890 nm. (The transmission dip at around 430 nm is not clearly resolved due to the proximity to silvers' SP resonance at around 350 nm.) The transmission minima at around 430 nm or 620 nm correspond to the SP resonances along the planes that are compressed of either air- or quartz-side surfaces of metal islands, respectively.^{7,12,13} The transmission dip at around 890 nm is ascribed to the SP resonance localized at each metal island, i.e., the resonance along the periphery of metal island surface.⁷

The wavelength that corresponds to an in-plane SP resonance can be expressed as follows:⁹

$$\lambda = \frac{d}{m} \operatorname{Re} \left(\sqrt{\frac{\varepsilon_d \varepsilon_m}{\varepsilon_d + \varepsilon_m}} \right), \quad (1)$$

where d is the grating period, m is the order of the grating vector involved, and ε_m and ε_d are the dielectric constants of metal and dielectric (air or quartz), respectively. It should be mentioned that this condition is valid for asymptotically small amount of perturbations, for example, infinitesimally shallow corrugations of metal surface or narrow slit width relative to the grating period. The annealing-induced change in the geometry and size of metal islands is expected to alter the SP resonance condition. As the slit width (i.e., air gap) increases for a given period of grating, the SP waves propagating along either side (air or quartz side) of the periodic structure will have an increasing presence in the air gap re-

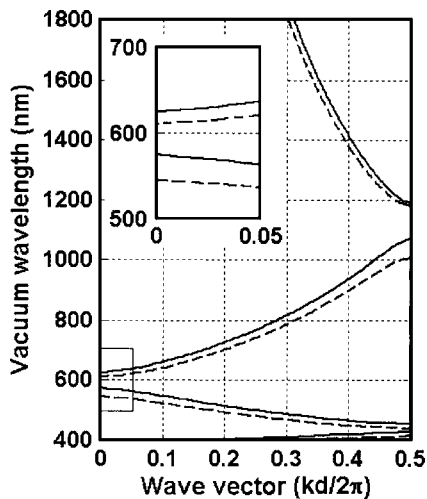


FIG. 3. Surface plasmon band structure calculated for a 1D silver nanoslit array structure with grating period of 400 nm: Slit width of 80 nm (solid curve) and 120 nm (dashed curve). The inset shows a magnified view of the band-gap opening around 600 nm wavelength.

gion. Since the free-space wave vector is smaller than the SP wave vector along the metal surface, the resonant wavelength is expected to blueshift with the increased air-gap portion. In the case of SP resonance localized to each island, a blueshift is also expected after annealing: The total periphery of each island decreases (as shown in the round cross section of metal islands), therefore, the corresponding resonant wavelength will decrease.

In order to substantiate the observed blueshift, we analyzed the energy band structure of SP waves interacting with the periodic metal/air gap structure. In the case of the in-plane SP waves propagating along the quartz-side surfaces of metal islands, the problem can be reduced to a one-dimensional (1D) periodic bilayer structure. Using the transfer matrix method, the following dispersion relation can be obtained between an in-plane SP wave vector k and the free-space wavelength λ_0 ¹⁴

$$\begin{aligned} \cos(kd) &= \cos(k_0a)\cos[k_m(d-a)] \\ &- \frac{1}{2}\left(\frac{k_0}{k_m} + \frac{k_m}{k_0}\right)\sin(k_0a)\sin[k_m(d-a)], \end{aligned} \quad (2)$$

where a is the slit width (air gap) and d is the grating period. k_0 is the free-space wave vector, $2\pi/\lambda_0$. k_m is the SP wave vector in the metal region, expressed as follows.

$$k_m = \text{Re}\left(\sqrt{\frac{\epsilon_d\epsilon_m}{\epsilon_d + \epsilon_m}}\right)k_0, \quad (3)$$

Regimes where $|\cos(kd)| \ll 1$ correspond to real k and thus to propagating Bloch waves: When $|\cos(kd)| > 1$, however, k has an imaginary part so that the Bloch wave becomes evanescent, i.e., entering into a forbidden band regime. Figure 3 shows the band structure, λ_0 versus $\text{Re}(k)$, calculated for grating period d of 400 nm, and slit width a of 80 nm (solid curve) or 120 nm (dashed curve). (The dielectric constants of Ag and quartz used in this simulation are from Ref. 15. The slit width was chosen in this range based on the SEM cross-sectional images shown in Fig. 1.)¹⁶ Clear opening of band gap is observed at the wavelength around 600 nm. As the slit width increases, the band-gap blueshifts (with the longer-

wavelength edge moving from 630 nm to 610 nm). At this wavelength range, the light incident normal to the slit array surface excites SP waves, assisted by the first-order grating vectors $(+2\pi/d)$. The in-plane SP waves propagating the opposite directions resonantly couple to each other, assisted by the second-order grating vectors available in the same structure. A resonant interaction between the two counterpropagating SP waves results in the formation of standing waves along the in-plane propagation direction. There are two possible standing waves with different energies so that there is an energy gap in the modal dispersion.¹⁷ One may anticipate observing another band gap at around 1200 nm wavelength. This band-gap regime, however, cannot be reached in this experiment, since a beam normally incident to a grating (of period d) cannot excite the desired SP wave vectors $(\pm\pi/d)$. Overall, this band structure calculation confirms that the in-plane SP resonance point corresponds to the minimal point of far-field transmission of light through the slit array and also that the amount of blueshift observed in the transmission spectrum of an annealed sample is reasonable compared to the slit width increase observed with SEM.

In summary, we have anneal-treated silver nanoslit arrays in a vacuum and investigated its effects on the surface morphology of silver and the surface plasmon resonance characteristics: A clear blueshift (20 nm) of transmission spectra was observed after annealing at 150 °C. The observed blueshift correlates well with the geometrical and dimensional changes of silver islands and slits as revealed by SEM analysis: Increased grain sizes, smooth, and round surface profiles of metal, and increased slit width after the anneal treatment. This study offers an interesting approach to altering surface plasmon resonance characteristics and thus optical transmission properties of metal nanoslit arrays.

This work has been supported by the NSF NIRT (Grant No. ECS-0403865).

¹W. L. Barnes, A. Dereus, and T. W. Ebbesen, *Nature (London)* **424**, 824 (2003).

²J. A. Porto, F. J. Garcia-Vidal, and J. B. Pendry, *Phys. Rev. Lett.* **83**, 2845 (1999).

³F. J. Garcia-Vidal and L. Martin-Moreno, *Phys. Rev. B* **66**, 155412 (2002).

⁴Q. Cao and P. Lalanne, *Phys. Rev. Lett.* **88**, 057403 (2002).

⁵M. M. J. Treacy, *Phys. Rev. B* **66**, 195105 (2002).

⁶Z. Sun and H. K. Kim, *Appl. Phys. Lett.* **85**, 642 (2004).

⁷Z. Sun, Y. S. Jung, and H. K. Kim, *Appl. Phys. Lett.* **83**, 3021 (2003).

⁸Z. Sun, Y. S. Jung, and H. K. Kim, *Appl. Phys. Lett.* **86**, 023111 (2005).

⁹H. Raether, *Surface Plasmons*, edited by G. Hohler (Springer, Berlin, 1988).

¹⁰J. I. Goldstein, A. D. Romig, Jr., D. E. Newbury, C. E. Lyman, P. Echlin, C. Fiori, D. C. Joy, and E. Lifshin, *Scanning Electron Microscopy and X-ray Microanalysis* (Plenum, New York, 1992), p. 200.

¹¹C. V. Thompson, *Annu. Rev. Mater. Sci.* **30**, 159 (2000).

¹²P. Lalanne, C. Sauvan, J. P. Hugonin, J. C. Rodier, and P. Chavel, *Phys. Rev. B* **68**, 125404 (2003).

¹³Y. Xie, A. R. Zakharian, J. V. Moloney, and M. Mansuripur, *Opt. Express* **13**, 4485 (2005).

¹⁴P. Yeh, *Optical Waves in Layered Media* (Wiley, Hoboken, 1998), p. 118.

¹⁵*Handbook of Optical Constants of Solids*, edited by E. D. Palik (Academic, New York, 1998).

¹⁶Due to the rather complex geometry of the metal's cross section, it is not straightforward to read the slit width, and this number is considered effective slit width measured at the metal/quartz interfaces.

¹⁷W. L. Barnes, T. W. Preist, S. C. Kitson, and J. R. Sambles, *Phys. Rev. B* **54**, 6227 (1996).